Characterization of the Electron Movement in Varying Magnetic Fields and the Resulting Anomalous Erosion

G. Buyle, D. Depla, K. Eufinger, J. Haemers, and R. De Gryse, Ghent University, Ghent, Belgium; and W. De Bosscher, Bekaert Advanced Coatings (Bekaert VDS), Deinze, Belgium

Key Words: Sputter deposition; Large area coating; Plasma simulation; DC magnetron plasma

ABSTRACT

The ionization along the magnet array in large sputter magnetrons with magnetic field gradients is simulated. Therefore, an analytical model is developed. The model is based on the collisionless orbits of the high energy electrons (HEE) and uses recurrent relations to determine the properties of the orbit with collisions from the orbit without collisions.

The simulations show that collisionless HEE orbits express transient behavior in a region with a magnetic field gradient. For example, the average height above the target of the electrons increases when the electron drifts from a weak to a strong magnetic field, although for constant magnetic fields the average height decreases with increasing magnetic field. The HEE are responsible for the ionization in the magnetron discharge. Hence, this transient behavior gives rise to anomalous ionization and (subsequently) erosion. The anomalous erosion in straight sections with a magnetic field gradient is simulated. The results show that the anomalous erosion depends on the absolute difference between the strong and weak magnetic field and on the length of the magnetic field gradient.

INTRODUCTION

Over the last decades, magnetron sputtering has become one of the most important methods for the deposition of thin films on large area substrates. In spite of its advantages, there remain some difficulties with the technique. One of them is the anomalous erosion that can occur at the ends of the target, or the so-called cross-corner effect. According to simulations [1-3], this effect can be attributed to a change in the electron drift velocity when the electrons move through a region with a magnetic field gradient. Hence, a magnetic field gradient leads to transient behavior of the electrons. In spite of this transient behavior, tuning of the magnetic field in the straight sections of a large magnetron allows for improvement of the uniformity of the deposited films. Increasing/decreasing the magnetic field at a certain position increases/decreases the deposition, and hence, also the erosion at that position. The main difference between the magnetic field gradients encountered in the straight sections and in the end sections of large magnetrons is the magnitude of the gradient. For magnetic field tuning typical gradients are in the order of 100 Gauss per meter [4], whereas at the ends, gradients more than 10 times as strong are encountered [1,3].

In this article we simulate the effect of a magnetic field gradient on the normalized ionization in a magnetron. An analytical model is developed for the determination of the ionization. This model, and the Monte Carlo model that was used to verify the model, are discussed in the next part. Then, the behavior of an electron orbit in a region with a magnetic field gradient is discussed. Afterwards, the results concerning the normalized ionization and normalized erosion rate are presented.

MODEL

The aim is to determine the ionization along the *y*-axis of the electrons emitted at the target. Therefore, two different models are used: a MC Model (MM) and an analytical model (AM). In the models only the high energy electrons are considered. First, the geometry of the model and the calculation of the collisionless electron orbits are discussed. Then, both the MM and the AM are explained.

Geometry and Collisionless Electron Orbits

The configuration used for the simulations is given in Figure 1. Part *a* of the figure shows a two-dimensional cross section, part *b* a top view. The dots represent possible starting positions of secondary electrons at the target. The term secondary electrons (SE) is used here for the electrons emitted from the target due to ion bombardment. In the direction along the magnet array (*y*-direction) the magnetic field can vary in strength. The magnetic field (B) is calculated by introducing so-called magnetic charges [5]. The electric field (E) is determined by the discharge voltage V_d, the cathode sheath thickness d_E and the assumption that the electric field varies linearly in the cathode sheath. Both V_d and d_E are considered as input parameters.

 505/856-7188 ISSN 0737-5921

47th Annual Technical Conference Proceedings (April 24–29, 2004) Dallas, TX USA

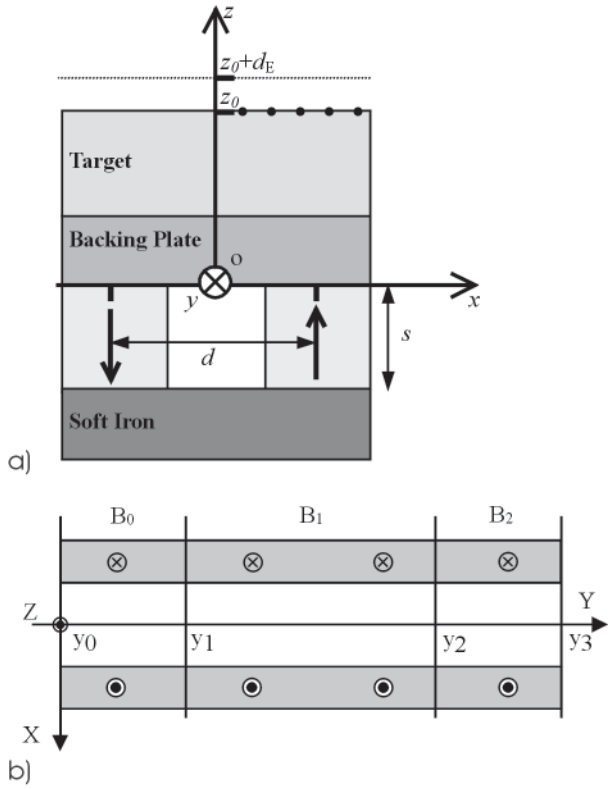

Figure 1: Sketch of the magnetron model. a) 2D cross section showing the magnets with side length *s* (12 mm) and distance *d* (36 mm) between them, placed on a soft iron plate. The target surface is at z_0 (15 mm). The thickness of the cathode sheath d_E is 1.0 mm. b) Top view of the magnet array. Different magnetic field strengths are possible along the *y*-axis.

The collisionless orbit of an electron in an electric and magnetic field is described by the Lorentz equation:

$$\frac{d\mathbf{v}}{dt} = \frac{q}{m}(\mathbf{E} + \mathbf{v} \times \mathbf{B})$$

Equation 1

with *q*, *m* and *v* the electric charge, mass, and velocity of the electron, respectively. This equation is solved numerically using a Runge-Kutta scheme. The time step δt to solve the equation is 2 x 10^{-11}s.

Monte Carlo Model (MM)

When a SE is emitted from the target, it is accelerated over the cathode sheath and becomes a high energy electron (HEE). If the HEE is not recaptured by the target, it will interact with the discharge gas [6]. Because of these interactions, it will lose energy. When its energy drops below a certain threshold energy E_{th}, it is not considered a HEE anymore. The determination of the ionization of the HEE is rather straightforward using a MC scheme. The method used will only be summarized here as it is described in more detail elsewhere [7]. The basis is solving the Lorentz equation (see previous section). For determining the ionization, it needs to be checked per δt whether a collision occurs or not. If a collision occurs, its type is determined. The cross-sections as found in [8] are used. For an excitation, the energy of the HEE is reduced with 11eV, for an ionization with 16eV. The HEE is followed until its energy drops below E_{th} or until it reaches the edges of the computational domain. The *y*-axis is split in intervals Y_i, each with length ΔY. The number of ionizations per Y_i is recorded. This way the ionization along the *y*-axis of a SE emitted at a certain position is retrieved.

Analytical Model (AM)

The first step in the AM is the calculation of the collisionless orbit of a SE (discussed earlier). While retracing the orbit, the time T_i needed to travel through the interval Y_i is recorded together with S_i, the distance the electron travels to pass through Y_i. This distance is longer than ΔY because of the gyration of the electron around the magnetic field lines. From T_i and S_i the kinetic (U_i) and potential (V_i) energy is calculated. We deduce two recurrent relations to determine in each interval Y_i the properties of the orbit with collisions from the properties of the orbit without collisions. The first is the relation for the energy $E_{c,i}$ of the electron:

$$E_{c,i+1} = E_{c,i} - \Delta E_i$$

Equation 2

with ΔE_i the energy lost by the HEE in interval Y_i because of interactions with the gas. The properties of the electron orbit with collisions, are indicated in this article with the index *c*, except for ΔE_i because this quantity does not apply to the collisionless orbit as it is zero by definition. The start value $E_{c,0}$ of the recurrent relation is derived from the fact that the energy of the HEE in the first bin is equal to the maximum possible energy, i.e. $E_{c,0}=e|V_d|$. To determine the kinetic energy $U_{c,i}$ and the potential energy $V_{c,i}$ in interval Y_i, we assume that the ratio of the kinetic and potential energy remains constant. This ratio is determined from the collisionless orbit.

To determine the energy loss ΔE_i, we propose the following relation:

$$\Delta E_i = \frac{W T_{c,i}}{T_{ion,i}}$$

Equation 3

with W the effective ionization energy, $T_{c,i}$ the time the HEE needs to pass through Y_i and $T_{ion,i}$ the average time between two ionizations. The effective ionization energy W is the

average energy needed to create an electron-ion pair, taking into account that more energy is lost to other processes than ionization. The average time between two ionizations $T_{ion,i}$ is equal to the mean free path λ divided by the electron velocity. To determine ΔE_i from Equation 3 we still need to find $T_{c,i}$, i.e. the time the HEE needs to travel through bin Y_i. T_i is not equal to $T_{c,i}$: the first is the time needed to pass through Y_i for an orbit without collisions; the latter is the same property for an orbit with collisions. By definition is the drift velocity $u_{c,i}$ in interval Y_i given by $u_{c,i} = \Delta Y/T_{c,i}$. As the width ΔY of the intervals is constant, we find the second recurrent relation:

$$T_{c,i} = T_{c,i-1}\frac{u_{c,i-1}}{u_{c,i}}$$

Equation 4

The drift velocity $u_{c,i}$ is proportional with the total velocity $v_{c,i}$, which in turn is proportional with the square root of the kinetic energy $V_{c,i}$. Furthermore, the drift velocity is proportional with the electric field, which is proportional with the square root of the potential energy $U_{c,i}$ of the electron (because the potential energy is determined by the electric field). Thus, we find the relation:

$$T_{c,i} = T_{c,i-1}\frac{\sqrt{V_{c,i-1}U_{c,i-1}}}{\sqrt{V_{c,i}U_{c,i}}}$$

Equation 5

This relation assumes implicitly that the T_i of the collisionless orbit are equal. However, due to e.g. a change in the B-field, this is not always valid. Therefore, we need to include the factor T_i/T_{i-1} in the relation for $T_{c,i}$, which leads to:

$$T_{c,i} = T_{c,i-1}\frac{T_i}{T_{i-1}}\frac{\sqrt{V_{c,i-1}U_{c,i-1}}}{\sqrt{V_{c,i}U_{c,i}}}$$

Equation 6

Given that $E_{c,0} = e|V_d|$ (discussed earlier), it follows that $T_{c,0} = T_0$ with T_0 the time needed to pass the first interval for the collisionless orbit. As $T_{c,0}$ and $E_{c,0}$ are known, ΔE_0 can be calculated (Equation 3). From this, $E_{c,1}$ can be derived (Equation 2), and subsequently $T_{c,1}$ (Equation 6) and ΔE_1 (Equation 3). This way the properties of the orbit with collisions are determined. ΔE_i is in each interval proportional with the average energy lost due to ionizations because W is considered constant. Hence, the normalized ionization distribution of a HEE along the *y*-axis is in each interval Y_i proportional with ΔE_i.

RESULTS AND DISCUSSION

Drift Velocity of Collisionless Electron Orbits

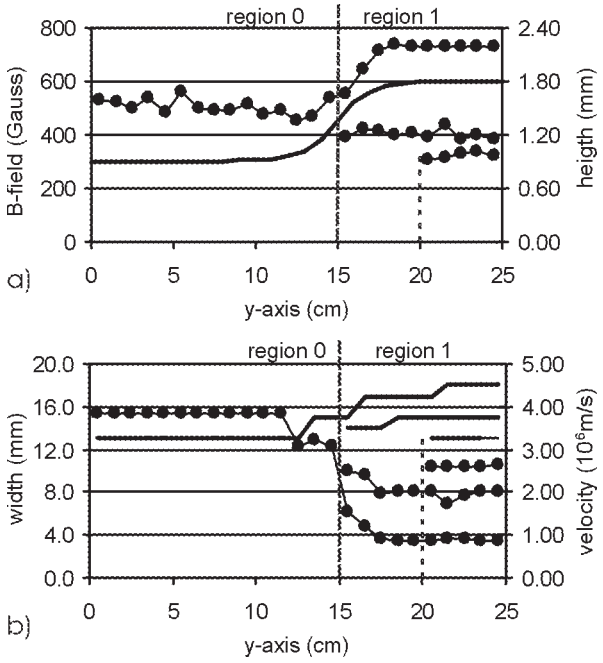

Figure 2. a) The magnetic field at the target surface along the *y*-axis (—). For secondary electrons emitted at *y* = 0, 15 and 20cm and *x* = -0.0625cm the average height above the target is plotted (•) on the right vertical axis. b) The width of these orbits (—) and the electron drift velocity (•) are shown on the left and right vertical axis, respectively.

First, we discuss the behavior of a collisionless electron orbit in a magnetic field gradient. Therefore, we consider a geometry as shown in Figure 1b but limit ourselves to the region between y_0 and y_2. We set y_0=0, y_1=15, y_2=25, V_d=-300V and d_E=1.0mm. These values for V_d and d_E are also used for all other results in this article. Be B_0 (B_1) the maximum horizontal magnetic field at the target surface in region 0 (region 1). The strength of the magnets is chosen such that B_0=300G and B_1=600G (Figure 2a). A secondary electron (SE) is emitted from the position *x*=-0.625 for *y*=0, 15 and 20. Its collisionless orbit is retraced until it reaches y_2=25 (Figure 2a). The average height *h* in region 0 of an electron emitted in region 0 (at *y*=0) is approximately 1.6mm. Similarly, *h* is approximately 1.0 mm in region 1 for an electron emitted in region 1 (at *y*=20). Nevertheless, the average height increases from 1.6 to 2.7 mm when the electron drifts from region 0 to region 1. Hence, there is a specific transition behavior. For the SE emitted at the edge between region 0 and 1 (at *y*=15), the effect is less but still visible. The width *w* of the orbit is determined by the *x*-value of the start position of the electron. Hence, *w* is the same regardless of whether the electron is emitted in the weak or strong magnetic field. However, when the electron drifts from

the weak to strong B-field, the width increases (Figure 2b). Also for the drift velocity u a transition behavior is observed (Figure 2b). The drift velocity of a SE that drifts from region 0 to region 1 decreases as expected, but it decreases so strongly that its drift velocity becomes lower than the drift velocity of a SE directly emitted in region 1. Thus, in this case there is an overcompensation which indicates that there is again a specific transition behavior. Analogue results are obtained for a transition from a strong to a weak field (not shown).

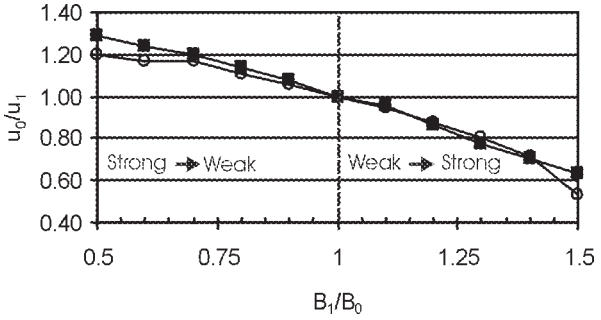

Figure 3: Plot of the ratio of the drift velocities u_0 and u_1 as a function of B_1/B_0, with u_0 (u_1) the drift velocity in region 1 of an electron emitted in region 0 (region 1). The results are shown for B_0=600G (■) and B_0= 300G (○).

To discuss more generally the influence of a magnetic field gradient, we focus on the drift velocity. Be u_0 the drift velocity in region 1 of a SE emitted in region 0 (at y=0) and u_1 the drift velocity in region 1 of a SE emitted in region 1 (at y=20). The ratio of u_0 and u_1 is plotted as a function of the ratio of the magnetic field strengths B_1 and B_0 (Figure 3). Values on the horizontal axis below one indicate a transition from a strong to a weak field, values larger than one transitions from a weak to a strong field. The figure contains the results obtained for both B_0=300G and for B_0=600G. From the figure it can be deduced that the relative change in the drift velocity is stronger for a transition from a weak to a strong than for a strong to a weak magnetic field. As the two curves are almost identical, it follows that the relative change in the magnetic field determines the change in drift velocity.

Normalized Ionization in Cyclic Configuration

For this part we use the geometry shown in Figure 1b with y_0=0, y_1=100, y_2=300, y_3=400, B_0=B_2=600G and B_1=300G. The resulting magnetic field is given in Figure 4. The width ΔY of the intervals along the y-axis is set to 5 cm. The strength of the magnets is chosen such that the width of the transition zone (TZ, the region with a magnetic field gradient) is equal to 10cm. The configuration is assumed cyclic: electrons that reach y_3 continue their orbit again at y_0. First, the ionization along the y-axis is determined using the MM: SE are emitted from x=-1.425, -1.325,…, -0.025 and per y-interval. Per starting position 30 electrons are emitted. The gas pressure is 0.5Pa, the effective ionization energy W is set to 20eV and the energy threshold E_{th} to 20eV. The resulting ionization distribution is also shown in Figure 4. The distribution is normalized, i.e. the total area under it is equal to one. There is an increased ionization after y_2 and a decreased ionization after y_1. Given the results obtained for the collisionless electron orbits (described earlier), these phenomena can be easily explained: the peak is due to the decrease in the electron drift velocity because at y_2 the electrons move from a weak to strong B-field, the dip is due to the increase in drift velocity because of the transition from a strong to a weak B-field at y_1.

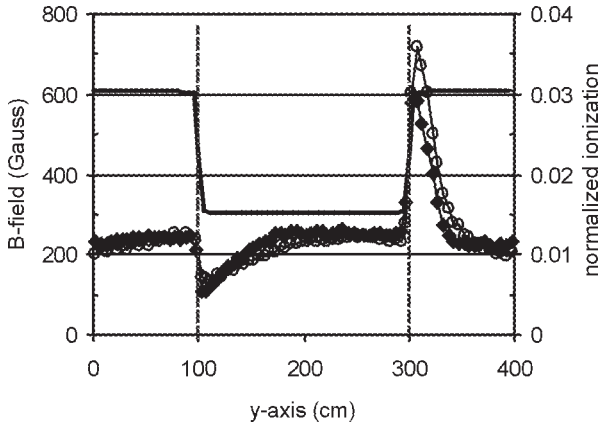

Figure 4: The magnetic field at the target surface along the y-axis (—). For the normalized ionization the solutions obtained with the Monte Carlo model (◆) and with the analytical model (○) are displayed (right vertical axis).

In Figure 4 the ionization obtained with the AM is also shown. As can be seen both methods agree rather well, and although the match is not exact, the AM is able to reproduce the general trend. In the MM, the ionization distribution of a SE emitted at a certain position is obtained by calculating it several times (30 for the result shown, as mentioned before). In the AM, the ionization distribution is based on the calculation of the collisionless orbit and this calculation needs to be done only once. Hence, the AM is much faster than the MM. Consequently, the results shown in the remaining part of the article are obtained using the AM.

The ionization distribution shown in Figure 4 is obtained for the condition that from all target positions the same amount of SE is emitted. Consequently, the ionization distribution in the region with the strong and weak magnetic field are the same. In reality, positions at the target with an increased ionization will have an increased ion bombardment and SE emission. To model this, we assume that the SE coefficient is constant and that all ions bombard the target at the y-value where they are created. The normalized amount of SE emitted at a given y-position is then proportional with the normalized ionization at that point. Hence, the obtained ionization distribution can be used as emission profile for the SE. This leads to an iteration

process, which reaches self-consistency after approximately 15 iterations (Figure 5). As can be seen, the peak value is less pronounced and more spread out in the final ionization profile. As expected, the ionization in the weak magnetic field is lower than in the strong magnetic field.

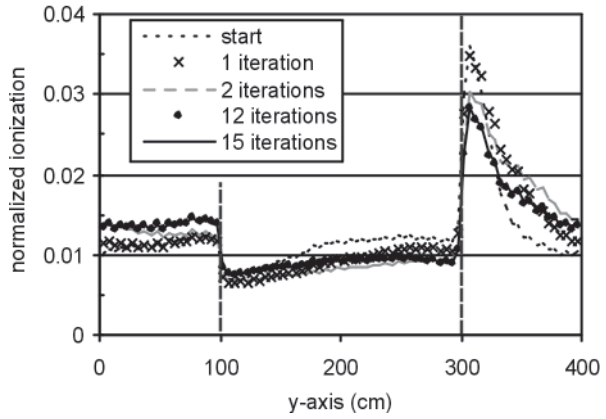

Figure 5: Effect of using the obtained normalized ionization as emission profile for the SE. A self-consistent solution is reached after approximately 15 iterations.

Application: Normalized Erosion Rate

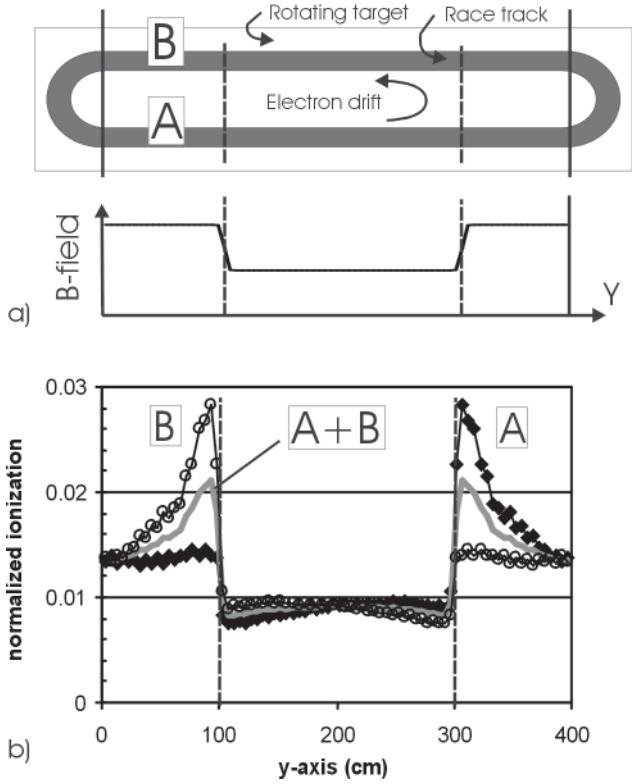

Figure 6: a) Sketch representing a rotating target with a race track on top. The straight parts A and B of the race track and the direction of the electron drift are indicated. b) The normalized ionization of part A (◆), part B (○) and their sum (—) along the *y*-axis. This sum is proportional with the erosion rate at the target surface.

So far, only a single straight magnet array was discussed. Now, we consider a whole magnetron configuration (Figure 6a), consisting of two straight parts (A and B) and the turns. The magnetic field configuration of the straight parts is taken the same as in the previous section. Hence, when the end effects are neglected, the ionization of part A is the same as the one obtained in the previous section (Figure 5). The ionization from part B can be easily derived from part A because they have the same magnetic field. The only difference is the direction of the drift velocity of the electrons. Both the ionization distributions of part A and B and their sum are shown in Figure 6b. To deduce the erosion rate from these ionization distributions, we adopt the earlier assumption that all ions bombard the target at the *y*-position where they are created. Furthermore, we assume a constant sputter yield (although it depends in reality on the energy of the incoming ion [9]). Given these assumptions, the normalized erosion rate is proportional with the normalized ionization at that point. For a rotating target, the erosion rate (ER) at point *y* is given by the sum of the ER of part A and B. Hence, the sum of the ionization distributions shown in Figure 6b is proportional with the normalized erosion rate at the target surface. The result confirms that magnetic field tuning is indeed effective, and the ER in the weak field is clearly lower than the ER in the strong field. However, the ratio of the erosion rates is larger than the ratio of the magnetic field strengths.

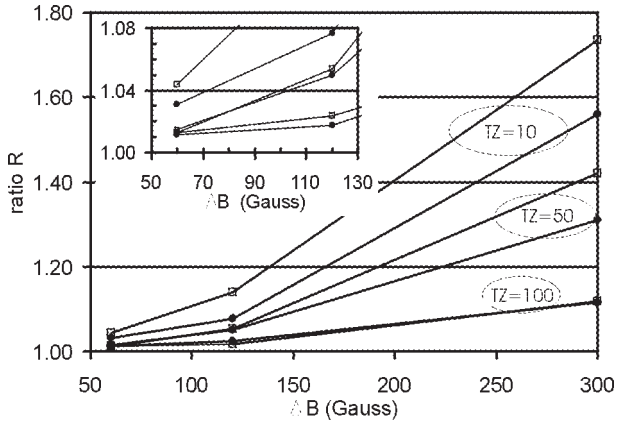

Figure 7: The ratio R as a function of ΔB. The influence of the width of the transition zone (TZ=10, 50 and 100 cm) is shown for both B_0=430G (□) and B_0=600G (●). The inset shows a detail of the region ΔB<130G.

Another important aspect is the anomalous erosion due the magnetic field gradient. To quantify this effect we introduce the ratio R, defined as ER_{peak}/ER_{strong} with ER_{peak} the peak value of ER and ER_{strong} the erosion rate in the strong B-field. Figure 7 shows the results for this ratio R calculated for two different maximum horizontal magnetic field strengths at the target (B_0=430 and 600G), for different ΔB (ΔB=B_0-B_1=60G, 120G and 300G) and for different lengths of the transition zone (TZ=10, 50 and 100cm). The situation shown in Figure 6b

corresponds with B_0=600G, ΔB=300G and TZ=10 cm and has R=1.74. The ratio R depends strongly on ΔB, the difference between B_0 and B_1, which could be expected. However, also the TZ and the absolute value of B_0 (or B_1) are important. This is illustrated by the fact that for B_0=430G the ratio R is smaller for ΔB=300G and TZ=100 cm than for ΔB=120G and TZ=10cm.

CONCLUSION

In this article the ionization along the magnets in large sputter magnetrons is simulated. Because of the large dimensions, a Monte Carlo approach becomes very time consuming. Therefore, an analytical model was developed. The model is based on the collisionless electron orbits and uses recurrent relations to determine the properties of the orbit with collisions from the orbits without collisions.

The simulations show that the HEE orbits express transient behavior in a region with a magnetic field gradient. Because of this the ionization and (subsequently) the erosion are influenced by a magnetic field gradient. The results show that the anomalous erosion depends on the absolute difference between the strong and weak magnetic field, on the length of the transition zone and on the absolute strength of the magnetic field.

ACKNOWLEDGMENT

This research is financed with a grant from the Institute for the Promotion of Innovation by Science and Technology in Flanders (IWT).

REFERENCES

1. E. Shidoji, M. Masaharu, and Takuji Nomura, "An anomalous erosion of a rectangular magnetron system", J. Vac. Sci. Technol. A. 18 (6), 2858, 2000.

2. A. Lopp, C. Braatz, M. Geisler, H. Claus, and J. Trube, "Plasma simulation for planar sputtering cathodes", 45th Annual Technical Conference Proceedings of the Society of Vacuum Coaters, ISSN 0737-5921, 170, 2002.

3. Q.H. Fan, L.Q. Zhou, and J.J. Gracio, "A cross-corner effect in a rectangular sputtering magnetron", J. Phys. D: Appl. Phys., 36, 244, 2003.

4. R. Dannenberg, R. Newcomb, and A. Ryan, "Uniformity Control of Rate Enhanced Reactive AC Sputtering", 42nd Annual Technical Conference Proceedings of the Society of Vacuum Coaters, 181, 1999.

5. W. Andrä et al., "Theoretical Aspects of Perpendicular Magnetic Recording Media", Phys. Stat. Sol. (a), 125, 9, 1991.

6. G. Buyle, W. De Bosscher, D. Depla, K. Eufinger, J. Haemers, and R. De Gryse, "Recapture of secondary electrons by the target in a DC planar magnetron discharge", Vacuum, 70, 29, 2003.

7. G. Buyle, D. Depla, K. Eufinger, J. Haemers, W. De Bosscher, and R. De Gryse, "Simplified model for calculating the pressure dependence of a direct current planar magnetron discharge", J. Vac. Sci. Technol. A. 21 (4), 1218, 2003.

8. J. Bretagne et al., "Relativistic electron-beam-produced plasmas. I: Collision cross sections and loss functions in argon", J. Phys. D: Appl. Phys. 19, 761, 1986.

9. N. Matsunami et al., "Energy dependence of the ion-induced sputtering yields of monoatomic solids", Atomic Data and Nuclear Data Tables, 31, 1, 1984.